Society For Biomaterials

Beneficial effects of hydrocortisone or spironolactone coating on foreign body response to mesh biomaterial in a mouse model

Christopher J. Brandt,[1] Daniel Kammer,[2] Anette Fiebeler,[3] Uwe Klinge[2]

[1]Surgical Department of the University Hospital of the UVA/AMC, 1105 AZ, Amsterdam, The Netherlands
[2]Surgical Department of the University Hospital of the RWTH Aachen, Germany
[3]Clinic for Nephrology at the Hannover Medical School, Germany

Received 4 December 2010; revised 8 April 2011; accepted 11 April 2011
Published online 23 August 2011 in Wiley Online Library (wileyonlinelibrary.com). DOI: 10.1002/jbm.a.33136

Abstract: Prosthetic reinforcements markedly reduce the risk of hernia recurrence. However, the implantation of meshes is related to an inflammatory foreign body reaction (FBR) with serious complications (i.e., persistent seroma, wound infection, mesh migration, entrapment, chronic pain). Adrenal hormones profoundly modify inflammatory response. Their effects on FBR however, remain ill defined. We therefore studied the FBR to polyvinylidenfluoride (PVDF) mesh material that was coated with four different substances: hydrocortisone (COR) or mifepristone (MIF), which respectively stimulate and block the glucocorticoid receptor, and aldosterone (ALD) or spironolactone (SPI), which respectively stimulate and block the mineralocorticoid receptor. The coated substances were released from the meshes within 24 h. Seven, 21, and 90 days after implantation, the specimen was evaluated for collagen formation, granuloma size, inflammatory activity, and angiogenesis. COR and SPI coating protected from inflammatory response, while ALD and MIF coating showed little difference to the control group. The COR and SPI groups showed smaller granuloma sizes at all time points, as well as a reduced number of inflammatory cells ($p < 0.001$) at day 90, and decreased collagen formation starting after 21 days ($p < 0.05$). There was a negative correlation for angiogenesis with inflammation around foreign body structures. In summary, these results suggest that early and temporary stimulation of the glucocorticoid receptor or blockade of the mineralocorticoid receptor have beneficial effects on FBR in the long term. © 2011 Wiley Periodicals, Inc. J Biomed Mater Res Part A: 99A: 335–343, 2011.

Key Words: glucocorticoid, mineralocorticoid, foreign body reaction, inflammation

How to cite this article: Brandt CJ, Kammer D, Fiebeler A, Klinge U. 2011. Beneficial effects of hydrocortisone or spironolactone coating on foreign body response to mesh biomaterial in a mouse model. J Biomed Mater Res Part A 2011:99A:335–343.

INTRODUCTION

The use of prosthetic mesh material is routine in the management of inguinal and incisional hernia in contemporary surgery.[1–3] Although prosthetic reinforcements markedly reduce the risk of recurrence, the implantation of alloplastic meshes is related to possible serious complications such as persistent seroma, wound infection, mesh migration, entrapment of structures in the cicatrix,[4] and subsequent chronic pain.[5,6]

These mesh-related complications are considered to be related to extensive local inflammation, which is the initial step of foreign body reaction (FBR).[4] FBR is initiated following the implantation of biomaterials, when locally damaged tissue secretes a wide variety of proteins that attract inflammatory cells to the site of the injury. A substantial proportion of these inflammatory cells is involved in the regulation of extracellular matrix (ECM) remodeling and collagen deposition.[7]

The crux, however, with foreign body implants is their permanent character, which can cause a persistent and increased inflammation with ongoing collagen deposition leading to extensive fibrosis and deteriorating the overall result.[8] It has been suggested that impaired host-acceptance of the implanted mesh will present itself through chronic inflammation and extensive fibrosis.[9] Eventually, a foreign body granuloma (FBG), consisting of concentrically deposited inflammatory cells imbedded in a thick fibrous capsule, will mark the area of implantation.

In attempts to tackle the problem of excessive FBR, some research groups have modified the chemical and physical properties of foreign body surfaces through coating, and have as a result shown altered local cell activation and tissue response.[10,11] Thus, the coating of polymer surfaces may pose an opportunity to improve mesh integration and biocompatibility.

As therapeutic drugs, corticosteroids have been utilized for their immunosuppressive benefits in daily practice for decades. The mineralocorticoid and glucocorticoid receptors have both been shown to change inflammatory and immunological activities.[12] Furthermore, recent emphasis on their effects on tissue remodeling and fibrosis in FBR underline their therapeutic potential.[6]

Correspondence to: U. Klinge; Department of Surgery, RWTH Aachen, Pauwelsstrasse 30, 52074 Aachen, Germany; e-mail: uklinge@ukaachen.de
Contract grant sponsor: European Section of the Aldosterone Council (ESAC) to D.K. and U.K.

Accordingly, we developed a mouse model to investigate the role of the mineralocorticoid- and glucocorticoid receptors in FBR around steroid-coated polyvinylidenfluoride (PVDF) meshes. As parameters of biocompatibility we considered the severity of inflammatory reaction, the extent of fibrosis with subsequent alterations of the ECM, and angiogenesis after 7, 21, and 90 days.

MATERIALS AND METHODS

Mesh materials and coating

The basic prosthetic material used for the construction of the four differently coated mesh samples was PVDF (FEG Textiltechnik, Aachen, Germany). The filaments had a diameter of 125 μm in a textile construction consisting of pores larger than 1000 μm. After plasma activation, acrylic acid was applied to the PVDF surface. Hydrocortisone (COR), aldosterone (ALD), spironolactone (SPI), and mifepristone (MIF) (substances all from Sigma-Aldrich, Steinheim, Germany) were dissolved in a gelatine/glycerine hydrogel. This solution was then sprayed onto the mesh.[13,14] *In vitro* measurements of release kinetics (done by the manufacturer) showed that the non-crosslinked hydrogel was dissolved in water within 1 h, thereby releasing the incorporated pharmaceutical. A serum measurement of the mice after 24 h was not done, not least because corresponding analyses were difficult to establish and interpret. Considering a tissue cube with a distance of 1 cm to mesh as most relevant area for the tissue response, and assuming a complete dissolution of the pharmaceutical, the following local concentrations were expected: an ALD load of 200 ng/cm^2 mesh corresponds to a concentration of 0.1 μg/cm^3; a SPI load of 40 μg/cm^2 mesh corresponds to 20 μg/cm^3; a COR load of 10 μg/ cm^2 mesh corresponds to 5 μg/cm^3; and a MIF load of 4 μg/cm^2 mesh corresponds to a concentration of 2 μg/cm^3.

Animals

A total of 68 male C57/BL6 mice (body weight 25–50 g) were housed under conditions of constant light and temperature and received a complete diet of mouse feed and water *ad libidum* throughout the entire study, which was performed in accordance with the guidelines of the "Deutsche Tierschutzgesetz" (50.203.2-AC 18, 29/01) and the National Institutes of Health (Bethesda, MD) for the use of laboratory animals. The animals were randomly divided into five groups consisting of PVDF (CONTROL), PVDF + SPI, PVDF + COR ($n = 14$), PVDF + ALD, and PVDF + MIF ($n = 13$). Subsequently, the animals were divided into 7, 21 ($n = 5$), and 90-day ($n = 3$ or 4) time points.

Surgical procedure

The operative procedure was performed under sterile conditions and general anesthesia by intramuscular administration of ketamine (10%; Sanofi-Ceva, Duesseldorf, Germany) and xylazine (Rompun 2%; Bayer, Leverkusen, Germany). Two paramedian full-thickness dermal incisions of 1.5 cm were made 1 cm distal to the xiphoid process. Subcutaneous sacs were then prepared laterally towards the flanks either as control, or to place a 1cm^2 mesh [Fig. 1(a)]. Skin closure was achieved with Prolene ® 5/0 sutures. After observation periods of 7, 21, and 90 days from implantation, animals were euthanized and the mesh with surrounding tissue was excised. Explants were fixed in 10% (pH 7.4) formalin for 24 h for immunohistochemical and morphological analysis.

Histological assessment

Histological and immunohistochemical investigations were performed on paraffin-embedded, 3-μm sections using the avidin-biotin-complex and diaminobenzidine as chromogen. All sections were stained with hematoxylin and eosin (H&E) and examined by standard light microscopy (Olympus BX51, Hamburg, Germany). For categorization of inflammatory cell density and for assessment of granuloma structure and size, we analyzed H&E stainings with digital imaging software (Image-Pro Plus; Media Cybernetics, Silver Springs). In addition, we stained macrophages and granulocytes to objectify inflammatory quantification. For the detection of macrophages we did a F4/80 staining, using monoclonal rat, 1:50 (Acris, Herford, Germany), as primary antibody and goat anti-rat, 1:50 (Dako, Glostrup, Denmark), as secondary antibody. For the detection of granulocytes, we did a myeloperoxidase staining, using rabbit polyclonal, 1:50 (Abcam, Cambridge, UK), as primary antibody and goat anti-rabbit, 1:50 (Abcam, Cambridge, UK), as secondary antibody (Fig. 2). For the detection of angiogenesis, immunohistochemical staining was performed for Von Willebrand Factor (F VIII; polyclonal rabbit, 1:500, DAKO, Glostrup, Denmark), followed by incubation with goat anti-rabbit IgG antibody (1:500, Dako). For cross-polymerization microscopy, 5 μm sections of the centre of the mesh samples and of the surrounding perifilamentary tissue were stained for 1 h in Picrosirius solution (0.1% solution of Sirius Red F3BA in saturated aqueous picric acid, pH 2) following the method of Junqueira et al. for staining of collagen types I and III.[15]

Regarding a considerable variation of tissue response within each section, we carefully defined areas for analysis, which were easy to comprehend for every investigator. The following criteria were assessed:

Category of inflammation. From the densest infiltrated area around each filament, the number of positively stained macrophages and granulocytes was calculated as a percentage of all cells in a 100 μm^2 area. The mean of these percentages was calculated and rated categorically into I1–I4 (1; <5%, 2; 5–30%, 3; 30–70%, 4; >70%) (Fig. 2). A minimum of six sections were examined per sample.

Granuloma size. Measurements of granuloma were performed on two muscular- and two fat-associated round filaments in the area with the lowest inflammation. Furthermore, the thinnest area of the granuloma was chosen for measurement of the cellular infiltrate (dense layer of inflammatory cells (>70%), bordering the filament) and reactive scar tissue (fibrotic capsule around filament containing 30–70% inflammatory cells).

Vascularization. Results were calculated as number of vessels/mm in a corridor with the width of the filament diameter (approximately 125 μm). The distance between

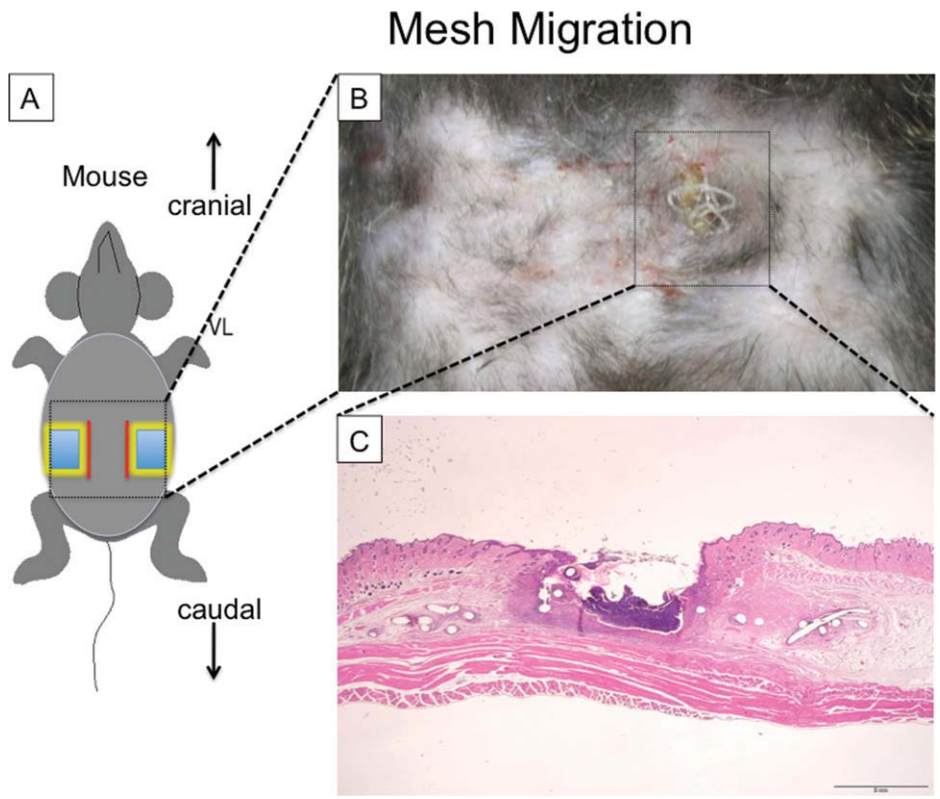

FIGURE 1. Schematic, photographic, and histological illustration of mesh migration. (A) Anatomic location of incision and insertion of squared meshes into subcutaneous skinfold. (B) Operation site after 90 days. The mesh structure has degraded and is macroscopically protruding the skin. (C) H&E staining illustrating mesh fibers migrating through the s.c. tissue and protruding the epidermis. The created porte d'entrée for pathogens, induces focal neutrophile granulocyte attraction (dark purple centre).

filaments and the minimum distance between filament and the first vessel were both calculated with previously mentioned imaging software.[6]

Collagen deposition. For each sample, standard regions within the interface (×400, area 100 × 100 μm directly next to the mesh fibers) were captured by a digital camera

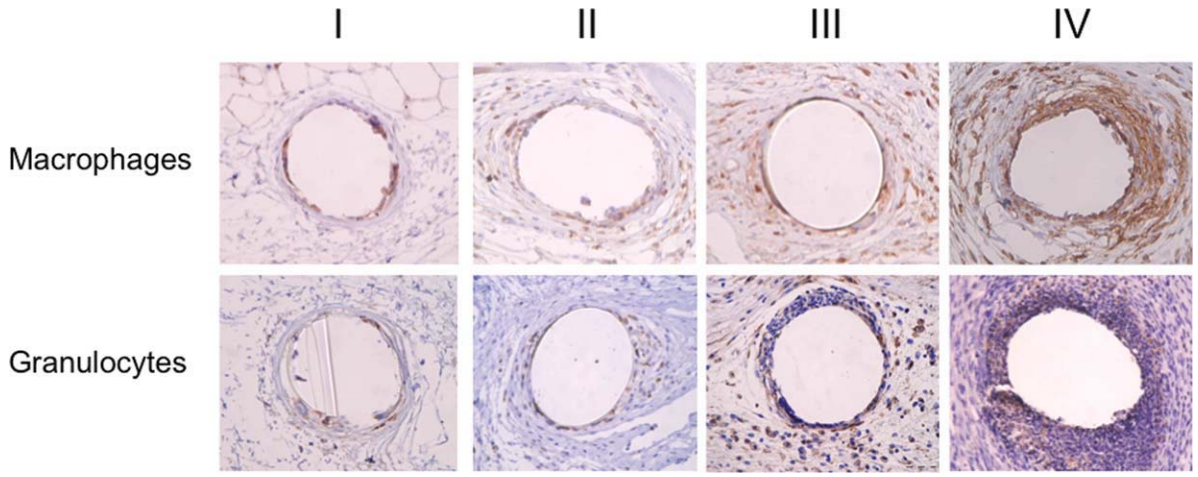

FIGURE 2. Depiction of inflammatory classification around PVDF mesh fibers after implantation in subcutaneous skinfold. Category 1 (I) shows low infiltration with a cell/ECM ratio of ± 1:5 and less than 20 cells/100 μm^2 area bordering the filament. Category 2 (II) describes moderate infiltration with a cell-ECM ratio of ± 1:3, and a cell count of 20–40 cells/100 μm^2 area bordering the filament. Category 3 (III) shows predominant infiltration with a cell-ECM ratio of ± 1:2 and a cell count of 40–60 per 100 μm^2 area bordering the filament. Category 4 (IV) portrays extensive infiltration with a cell-ECM ratio of ± 1:1, and a cell count of >60 cells/100 μm^2 area bordering the filament. Examination of macrophages done with F4/80 staining and detection of granulocytes done with myeloperoxidase staining, both at 200× magnification.

(C-3040; Olympus, Hamburg, Germany) while the deposition of collagen types I and III was obtained using digital image-analyzing software. For comparison of sections with the least dense collagen deposition, we selected the two roundest filaments with muscular association (i.e., <200 μm distance from muscle); the two roundest filaments with fatty association (i.e., >400 μm distance from muscle); and the two roundest filament-sets for analysis of interfilamentary collagen deposition (i.e., <200 μm distance from each other. To obtain the mean collagen deposition, the muscular-, fatty-, and interfilamentary-associated collagen deposition scores were added up and divided by 6. Collagen deposition is categorized into C1–C4 (Fig. 2).

Mesh Migration. Mesh migration was defined as any protrusion of mesh material through the skin after implantation periods of 7, 21, and 90 days.

Statistics

Statistical analyses were performed using the Statistical Package for the Social Sciences (SPSS). Data were organized according to types of coating and duration of implantation. Differences between the groups were evaluated for statistical significance by ANOVA. PostHoc rate-adjustment according to Bonferroni was performed in case of comparison between several groups. p-values < 0.05 were considered to be significant. All data are presented as mean values $\pm$ SEM. The granuloma size and the shortest distance from filament to vessel were both tested for normal distribution by the Kolmogoroff-Smirnov test.

RESULTS

All animals returned to normal activity after surgical intervention. There were no deaths during the postoperative observation periods. None of the mice showed signs of infection, hematoma, or other postoperative complications after 7 and 21 days. However, after 90 days, 9 out of 18 mice experienced mesh migration. Four out of four (100%) from the ALD group, two out of three (67%) from the MIF group, two out of five (40%) from the control group, one out of three (33%) from the COR group, and none from the SPI group (0%) showed mesh migration through the skin [Fig. 1 + Fig. 4(d); Chi^2 $p = 0.07$ between groups]. We found a generalized inhomogeneity of inflammatory intensity and collagen deposition within specimen. We also noted a significantly increased inflammatory reaction and increased size of FBG around mesh filaments in the vicinity of muscle in comparison with fatty association ($p < 0.05$).

Inflammation

After 7 days, we observed generalized inflammatory reaction around the mesh filaments in the control group with an inflammatory cell/ECM ratio of $0.33 \pm 1.5 \cdot 10^{-2}$ at the mesh interface. After 90 days, we found that this ratio increased to $0.5 \pm 3.2 \cdot 10^{-3}$ ($p < 0.05$). These inflammatory cells were identified as mainly granulocytes and macrophages (Fig. 2). While analyzing the effects of different coatings, we discovered significant similarities between COR and SPI and between ALD and MIF. There were no significant differences between the COR-SPI or the ALD-MIF groups with the control group at day 7 [Fig. 4(a)]. At day 21, only SPI had significantly reduced inflammation compared with the control group. At day 90, however, COR and SPI both showed significantly decreased inflammation compared with the control group, whereas the ALD-MIF groups showed little difference to the control group ($p < 0.001$).

Collagen deposition

At day 7, we saw a developing collagen structure in the control group with crossed orientation of most fibers. This consisted mainly of collagen type III (Fig. 3). After 21 days we noticed a significant increase in collagen I/III ratio and the development of thin bridging structures ($p < 0.05$). Even though collagen deposition continued into the 90-day time point, no significant increase was noted for the control group ($p = 0.182$).

Similar to the functional pairing of the drug groups in respect to inflammation, we found corresponding outcome for collagen deposition. Although at day 7 the outcome of neither group had differed significantly from the control group, by the 21 and 90-day time points COR-SPI showed decreased collagen deposition compared with the control group and the MIF-ALD group ($p < 0.05$) [Fig. 4(b)].

Granuloma size

In the control group, we found a steady growth of granulomas over time. Total granuloma size (mean of granuloma size in fatty tissue and with muscular association) increased from 48 ± 3.0 μm to 66 ± 3.7 μm ($p < 0.05$) between 7 and 21 days, and from 66 ± 3.7 μm to 106 ± 2.4 μm ($p < 0.001$) between 21 and 90 days. Although the increase in cellular infiltrate between 7 and 21 days was insignificant ($p = 0.126$), it did show substantial growth between 21 and 90 days ($p < 0.001$). The mean diameter of the reactive scar tissue, however, showed a significant increase over both intervals ($p < 0.001$).

Throughout the length of the study, we noticed that the COR and SPI groups behaved similarly with respect to mean granuloma size. The COR-SPI groups had significantly smaller mean granulomas in comparison with the control group at all three time points [Fig. 4(c)]. In contrast, MIF and ALD showed a similar increase only after 7 days, whereas at day 21 and day 90 only the ALD group exhibited a larger mean size. Interestingly, the effect of COR-SPI on mean granuloma size was mostly due to the decrease in reactive scar tissue, as it remained significantly reduced over all time points compared with the control group ($p < 0.05$). The effect of COR-SPI on the cellular infiltrate showed significant decrease only after 90 days ($p < 0.05$).

Neovascularization

The in-growth of new vessels increased over time, with a mean number of 9.1 ± 0.2 vessels/mm between filaments in the control group and a mean distance of 43 ± 0.9 μm between the filament and the nearest new blood vessel at 21 days (Table I). COR and SPI again acted significantly

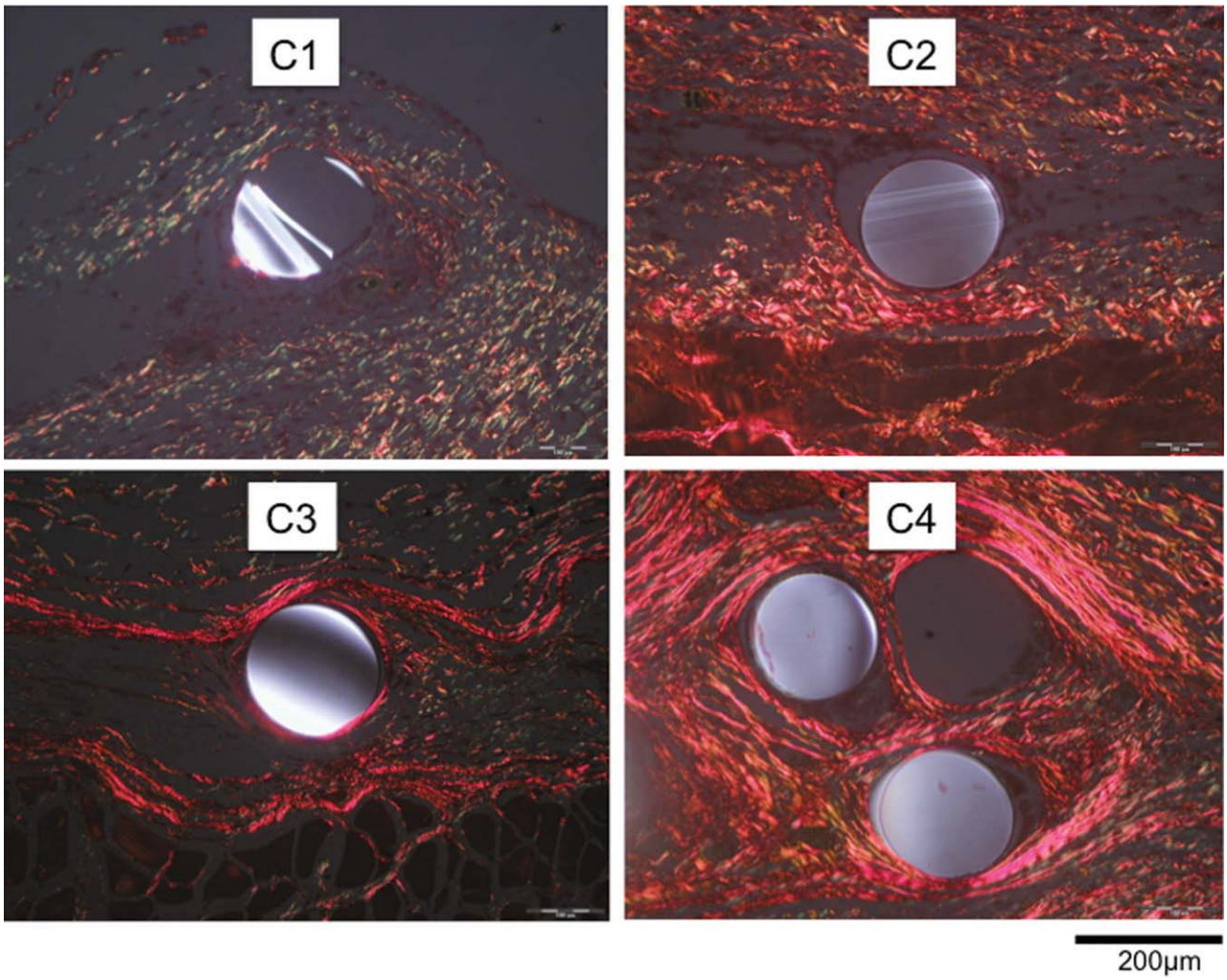

FIGURE 3. Categorization of collagen deposition around PVDF mesh fibers after implantation in subcutaneous skinfold. Category 1 (C1) represents scarce, collagen deposition, with crossed orientation of collagen fibers, which is non-circular around filament, and a collagen I/III ratio of <1:5. Category 2 (C2) shows moderate collagen deposition, which is circular around the filament, and has a crossed fiber orientation, with a collagen I/III ratio <1:5. Category 3 (C3) describes predominant collagen deposition with a thin bridging structure (<100 μm) between neighboring filaments but not circular around the filament, and a collagen I/III ratio >1:5. Category 4 (C4) represents severe collagen deposition with a thick bridging structure (>200 μm) between neighboring filaments and also circular around the filament, with a collagen I/III ratio >1:5. Examination done through cross polarization microscopy and Sirius red staining at 200× magnification. [Color figure can be viewed in the online issue, which is available at wileyonlinelibrary.com.]

similar in angiogenic proximity and quantity. With mean vessel counts of 13.2 ± 0.2 and 13.5 ± 0.3, respectively, and mean proximities of 21.5 ± 0.9 and 19.2 ± 0.9 μm to filaments, their angiogenesis was significantly increased in comparison with both the control group ($p < 0.001$) and ALD and MIF ($p < 0.001$) at day 21.

Collaboration network

Considering high correlation coefficients as indicator of close collaboration, we calculated Spearman's correlation coefficients and found significant positive correlations between inflammation and granuloma size ($r = 0.78$), between inflammation and collagen deposition ($r = 0.36$), and between granuloma size and collagen deposition ($r = 0.56$) (Fig. 5). We also calculated a negative correlation between inflammation and angiogenesis ($r = -0.63$), and between angiogenesis and collagen deposition ($r = -0.71$). Furthermore, we found that the type of coating significantly correlated to inflammation, but not to the other variables. ALD and MIF significantly enhanced inflammatory activity ($r = 0.36$ and $r = 0.22$, respectively) whereas SPI and COR decreased the inflammatory activity ($r = -0.47$ and $r = -0.31$, respectively).

DISCUSSION

The implantation of surgical biomaterials challenges the onset of a local inflammatory response syndrome (LIRS), which is a non-systemic reaction to sterile infliction (e.g., trauma, necrosis), a microbiological infection, or a combination of both.[16] Mesh-induced inflammation is linked to the size of the FBG with alteration in collagen composition[6]; thus it can be postulated that the level of inflammatory

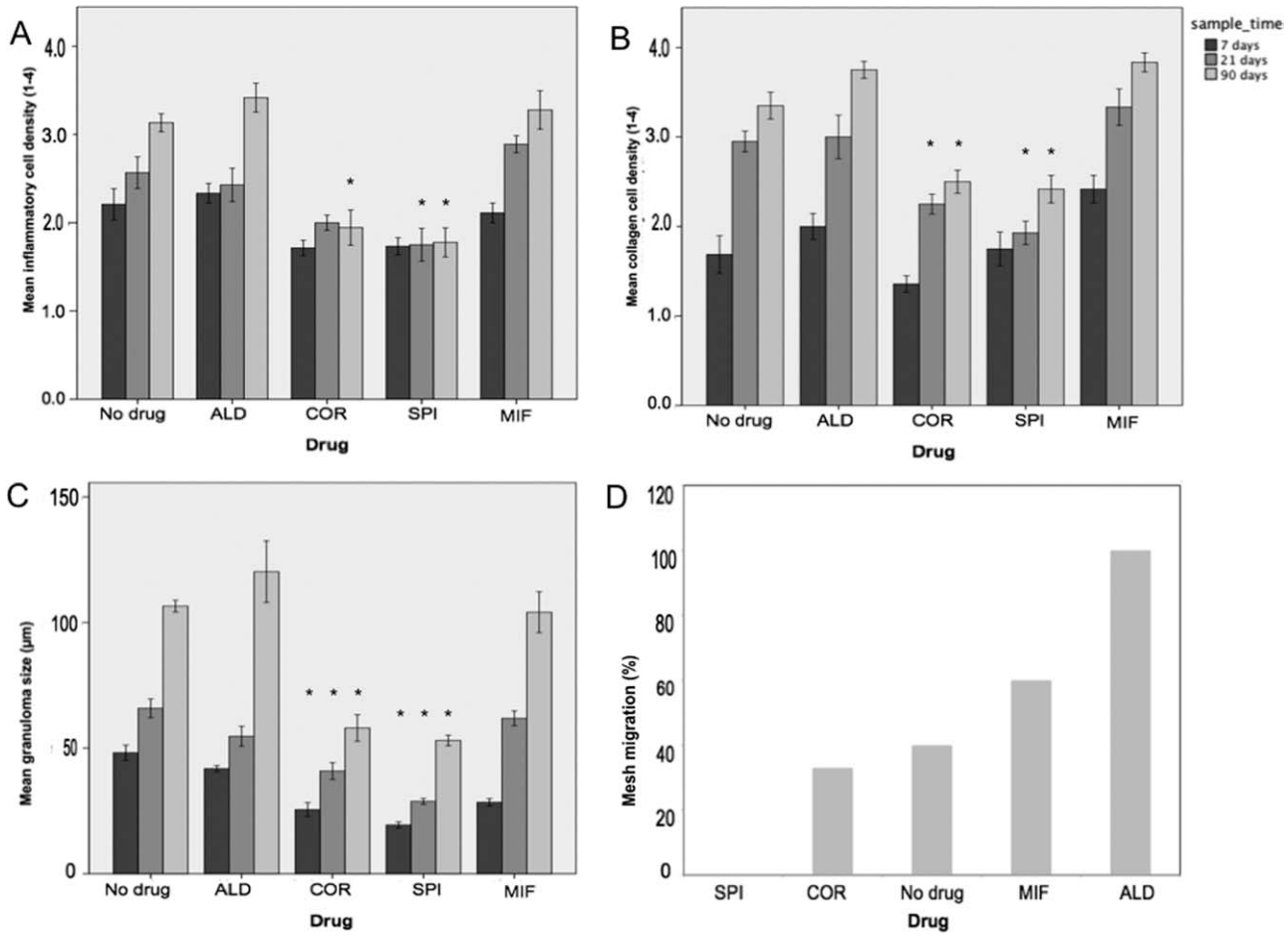

FIGURE 4. Histograms representing several histological alterations around mesh filaments coated with SPI, COR, ALD, MIF, and no drugs, over three time points (25 animals for analysis at days 7 and 21, and 18 at day 90). All data [except 4(D)] are presented as mean values ± SEM, $*p < 0.05$ vs. control group at corresponding time point. (A) Representation of mean inflammatory activity according to previously mentioned classification (I1–I4). (B) Representation of mean collagen density and structural formation, according to previously mentioned classification (C1–C4). (C) Depiction of mean granuloma size (µm), measured according to previously mentioned criteria. (D) Illustration of mesh migration per drug group after 90 days. Quantity of mesh migrations is shown as a percentage of the total amount of animals per group.

response is a major determinant of biocompatibility, and that addressing inflammation might reduce fibrosis around foreign body materials.

Studies done by Luttikhuizen et al.,[17] and Li et al.[11] demonstrate that the physicochemical structure of biomaterials controls inflammatory functions of macrophages (one of the inflammatory mediators) such as activation, adhesion, fusion, and programmed cell death, hereby determining the course of the FBR and subsequent biocompatibility. With our findings of modified inflammatory activity by local release of adrenal hormones we describe a novel way to interfere with the local inflammatory response, thereby triggering local wound healing and gaining beneficial long-term results on foreign body tolerance. In this regard we also interpret our observation of a negative correlation for angiogenesis in inflamed tissue around foreign body structures, which has not been described previously. One explanation for this negative correlation lies in the conflicting angiogenic properties of macrophages. It has been shown that so-called

TABLE I. Two Parameters of Neovascularization for the Different Coatings at day 21.

Applied Drug	Mean Vessel Count/1000 µm	Shortest Distance to Vessel (µm)
Control	9 ± 0.6	43 ± 2.9#
MR+	8 ± 0.4	48 ± 1.8#
GR+	13 ± 0.5*	22 ± 2.1
MR−	14 ± 0.9*	19 ± 2.4
GR−	7 ± 0.5	49 ± 1.7#

The mean vessel count per 1000 µm between mesh filaments, and the closest proximity of a vessel to the mesh interface were calculated through previously mentioned digital imaging software. (analysis was done through histological assessment of von willebrand factor treated coupes at 200× microscopical magnification.)

Values are shown as means ± SEM.

Calculation of significance between groups was done according to ANOVA with post hoc Bonferroni,

$*p < 0.05$ versus MR+, GR−,

$\#p < 0.05$ versus GR+, MR−.

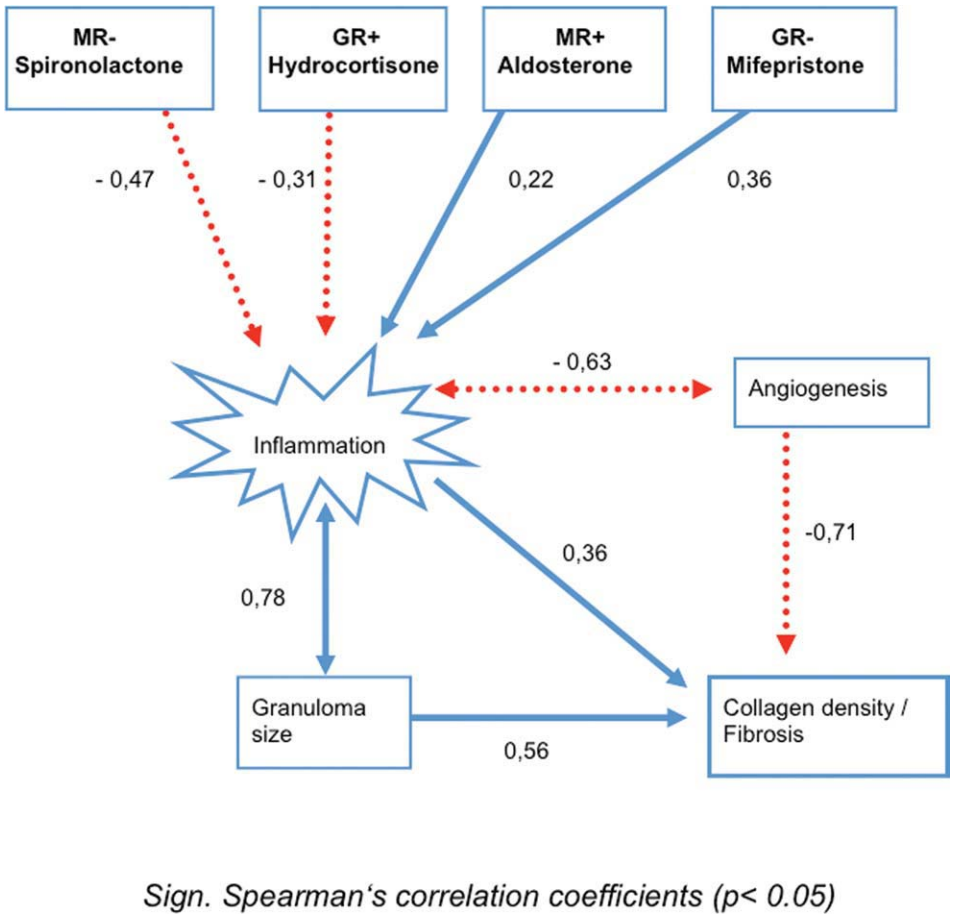

FIGURE 5. Depiction of significant Spearman correlation coefficients ($p < 0.05$) between histological parameters in reaction to s.c. mesh implantation, and the influence of different coatings on these parameters. [Color figure can be viewed in the online issue, which is available at wileyonlinelibrary.com.]

M1 macrophages are able to inhibit angiogenesis by instigating the programmed cell death of endothelial cells, after which they undergo differentiation into M2 macrophages.[18] M2 macrophages stimulate the formation of new vessels through the release of growth factors.[19] Although the molecular pathways are yet to be determined, it is likely that the modulation of inflammation through the mineralocorticoid and glucocorticoid receptor pathways has the potential to alter angiogenic induction by means of influencing the differentiation of M1 into M2 macrophages or interacting directly with these subtypes.

It has been known for decades that stimulation of the glucocorticoid receptor by COR decreases inflammation.[20] More recently, a growing number of experimental and clinical studies have demonstrated that stimulation of the mineralocorticoid receptor through ALD induces inflammation and tissue remodeling, and that blockage of this receptor with SPI inhibits inflammatory markers and profibrotic proteins.[21,22] Our study has been the first to compare the effects of the mineralocorticoid and glucocorticoid receptors on FBR around surgical mesh material. We found similar effects on tissue response for COR and SPI in comparison with the reciprocal effects exhibited by their functional opposites ALD and MIF. Supporting the functional similarity of the mineralocorticoid and glucocorticoid receptors in the inflammatory process, Bitar et al.[23] and Rickard et al.[24] showed inverted inflammatory responses to both stimulation and blockage of the glucocorticoid and mineralocorticoid receptor pathways. Conclusively, SPI, or the mineralocorticoid receptor-blocker eplerenone, which has also been shown to reverse established inflammatory and fibrotic responses,[25] might offer a novel strategy for immune-modification of biomaterials with possible beneficial effects on remodeling and integration of foreign materials.

The inflicted injuries in our study are limited peripheral injuries. An interesting question remains as to what extent this local injury can stimulate the central renin-angiotensin-aldosterone-system (RAAS), which enhances sympathetic activity and subsequently releases pro-inflammatory cytokines into the circulation, hereby worsening effects on peripheral injury, as described by Felder.[26] On activation of this axis, one might speculate on a beneficial effect of mineralocorticoid receptor-blockers to reduce such an inflammatory response. This would have to be investigated in a separate set of experiments.

Shahbaz et al.[27] point to the fact that ALD-induced inflammation is accompanied by a dyshomeostasis of macro- and micronutrients, which induces oxidative stress and impaired antioxidant defense, thereby leading to structural remodeling and fibrosis. In accordance we observed an intensified inflammation, accompanied by substantially increased fibrosis, in the presence of ALD. SPI, on the other hand, appears to moderate this cascade.

Previous approaches to coat mesh surfaces have also shown favorable effects on foreign body tolerance in animal models. In a transgenic mice model, Junge et al.[13] showed an increased biocompatibility of mesh materials that were modified with the antibiotic gentamicin. Despite its rapid release within 4 h they found improved collagen type I/III ratios after 21 and 90 days. More macroscopic results on intra-abdominal host response were described by Pierce et al.[28] after initial mesh-coating with Ω-3 fatty acids. In a rabbit model, they demonstrated decreased mesh contraction and visceral adhesions up to 120 days. In patients with cardiac stent re-stenosis, Scheller et al.[29] demonstrated that drug-coated balloon catheters, which release most of the drug within the first minute, prevent neointimal proliferation and restenosis after a follow-up of 12 months. In patients with coronary heart disease, Sgueglia et al.[30] have recently shown prevention from neointimal hyperplasia up to 12 months after single-shot paclitaxel application by second-generation drug-eluting balloon catheters in patients with coronary bifurcation lesions. Accordingly, we show that despite the rapid diffusion of the coated steroid hormones within 1 day, there is a strong correlation between the extent of the initial inflammatory response and subsequent morphological alterations such as development of fibrosis and angiogenesis.

Animal experiments have their natural limitations and the results cannot be directly projected onto humans. The general benefit, however, is improvement of the understanding of complex tissue response around implanted meshes under standardized conditions *in vivo*. Also, pharmacokinetics is difficult to control after implantation and may exhibit possible variations of the tissue response. Based on a hypothetical assessment, we attempted to mimic physiological blood-drug concentrations in a subcutaneous tissue radius of 1 cm^3 around the mesh, although the actual tissue concentration and diffusion radius may differ. Furthermore, in assessing the extent of inflammation and collagen deposition, we observed relative inhomogeneous tissue reaction within specimen. To avoid a possibly biased outcome, we standardized our choice of granulomas for analysis, corresponding with previously described criteria.

CONCLUSIONS

Early modification of adrenal hormone receptor activity can attenuate local inflammatory response to foreign bodies with subsequent beneficial long-term effects. In particular, stimulation of the glucocorticoid receptor or blockade of the mineralocorticoid receptor has protective potential. Further investigations should clarify dose response, the protective potential of a combination of both protective substances, and whether similar effects could be achieved by systemic delivery of drugs. In addition, we suggest extending our experimental protocol to other foreign material, such as stents or permanent catheters to improve their biocompatibility.

ACKNOWLEDGMENTS

The authors thank Ellen Krott for her excellent technical assistance.

REFERENCES

1. Bellon JM, López-Hervás P, Rodríguez M, García-Honduvilla N, Pascual G, Buján J. Midline abdominal wall closure: A new prophylactic mesh concept. J Am Coll Surg 2006;203:490–497.
2. Burger JW, Luijendijk RW, Hop WC, Halm JA, Verdaasdonk EG, Jeekel J. Long-term follow-up of a randomized controlled trial of suture versus mesh repair of incisional hernia. Ann Surg 2004; 240:578–83, discussion 583–585.
3. Luijendijk RW, Hop WC, van den Tol MP, de Lange DC, Braaksma MM, IJzermans JN, Boelhouwer RU, de Vries BC, Salu MK, Wereldsma JC, Bruijninckx CM, Jeekel J. A comparison of suture repair with mesh repair for incisional hernia. N Engl J Med 2000; 343:392–398.
4. Shin D, Lipshultz LI, Goldstein M, Barmé GA, Fuchs EF, Nagler HM, McCallum SW, Niederberger CS, Schoor RA, Brugh VM 3rd, Honig SC. Herniorrhaphy with polypropylene mesh causing inguinal vasal obstruction: A preventable cause of obstructive azoospermia. Ann Surg 2005;241:553–558.
5. Klinge U, Klosterhalfen B, Birkenhauer V, Junge K, Conze J, Schumpelick V. Impact of polymer pore size on the interface scar formation in a rat model. J Surg Res 2002;103:208–214.
6. Klinge U, Theuer S, Krott E, Fiebeler A. Absence of circulating aldosterone attenuates foreign body reaction around surgical sutures. Langenbecks Arch Surg 2010;395:429–435.
7. Eckes B, Zigrino P, Kessler D, Holtkötter O, Shephard P, Mauch C, Krieg T. Fibroblast-matrix interactions in wound healing and fibrosis. Matrix Biol 2000;19:325–332.
8. Setzen G, Williams EF III. Tissue response to suture materials implanted subcutaneously in a rabbit model. Plast Reconstr Surg 1997;100:1788–1795.
9. Klinge U, Klosterhalfen B, Müller M, Schumpelick V. Foreign body reaction to meshes used for the repair of abdominal wall hernias. Eur J Surg 1999;165:665–673.
10. MacEwan MR, Brodbeck WG, Matsuda WG, Anderson JM. Student Research Award in the Undergraduate Degree Candidate category, 30th Annual Meeting of the Society for Biomaterials. Memphis, Tennessee, April 27–30, 2005. Monocyte/lymphocyte interactions and the foreign body response: In vitro effects of biomaterial surface chemistry. J Biomed Mater Res A 2005;74:285–293.
11. Li X, Wang J, Yin Y, Luo C, Yao K. [Advances in interaction of macrophages with tissue engineering related biomaterials]. Sheng Wu Yi Xue Gong Cheng Xue Za Zhi 2008;25:487–490.
12. Han SY, Kim CH, Kim HS, Jee YH, Song HK, Lee MH, Han KH, Kim HK, Kang YS, Han JYl, Kim YS, Cha DR. Spironolactone prevents diabetic nephropathy through an anti-inflammatory mechanism in type 2 diabetic rats. J Am Soc Nephrol 2006;17: 1362–1372.
13. Junge K, Klinge U, Rosch R, Lynen P, Binnenbosel M, Conze J, Mertens PR, Schwab R, Schumpelick V. Improved collagen type I/III ratio at the interface of gentamicin-supplemented polyvinylidenfluoride mesh materials. Langenbecks Arch Surg 2007;392: 465–471.
14. Gupta B, Hilborn JG, Bisson I, Frey P. Plasma-induced graft polymerization of acrylic acid onto poly(ethylene terephthalate) films: Characterization and human smooth muscle cell growth on grafted films. Biomaterials 2002;23:863–871.
15. Junqueira LC, Cossermelli W, Brentani R. Differential staining of collagens type I, II and III by Sirius Red and polarization microscopy. Arch Histol Jpn 1978;41:267–274.
16. Legrand M, Klijn E, Payen D, Ince C. The response of the host microcirculation to bacterial sepsis: Does the pathogen matter? J Mol Med 2010;88:127–133.

17. Luttikhuizen DT, Harmsen MC, Van Luyn, MJ. Cellular and molecular dynamics in the foreign body reaction. Tissue Eng 2006;12: 1955–1970.
18. Pelegrin P, Surprenant A. Dynamics of macrophage polarization reveal new mechanism to inhibit IL-1beta release through pyrophosphates. EMBO J 2009;28:2114–2127.
19. Schmidt T, Carmeliet P. Blood-vessel formation: Bridges that guide and unite. Nature 2010;465:697–699.
20. de Scheerder I, Wang K, Wilczek K, van Dorpe J, Verbeken E, Desmet W, Schacht E, Piessens J. Local methylprednisolone inhibition of foreign body response to coated intracoronary stents. Coron Artery Dis 1996;7:161–166.
21. Han KH, Kang YS, Han S-Y, Jee YH, Lee MH, Han JY, Kim HK, Kim YS, Cha DR. Spironolactone ameliorates renal injury and connective tissue growth factor expression in type II diabetic rats. Kidney Int 2006;70:111–120.
22. Fiebeler A, Muller DN, Shagdarsuren E, Luft FC. Aldosterone, mineralocorticoid receptors, and vascular inflammation. Curr Opin Nephrol Hypertens 2007;16:134–142.
23. Bitar MS, Farook MS, Wahid S, Francis IM. Glucocorticoid-dependent impairment of wound healing in experimental diabetes: Amelioration by adrenalectomy and RU 486. J Surg Res 1999;82: 234–243.
24. Rickard AJ, Funder JW, Morgan J, Fuller PJ, Young MJ. Does glucocorticoid receptor blockade exacerbate tissue damage after mineralocorticoid/salt administration? Endocrinology 2007;148: 4829–4835.
25. Young M, Funder JW. Eplerenone, but not steroid withdrawal, reverses cardiac fibrosis in deoxycorticosterone/salt-treated rats. Endocrinology 2004;145:3153–3157.
26. Kang YM, Zhang Z, Johnson RF, Yu Y, Beltz T, Johnson AK, Weiss RM, Felder RB. Novel effect of mineralocorticoid receptor antagonism to reduce proinflammatory cytokines and hypothalamic activation in rats with ischemia-induced heart failure. Circ Res 2006;99:758–766.
27. Shahbaz AU, Sun Y, Bhattacharya SK, Ahokas RA, Gerling IC, McGee JE, Weber KT. Fibrosis in hypertensive heart disease: Molecular pathways and cardioprotective strategies. J Hypertens 2010;28(Suppl 1):S25–S32.
28. Pierce RA, Perrone JM, Nimeri A, Sexton JA, Walcutt J, Frisella MM, Matthews BD. 120-day comparative analysis of adhesion grade and quantity, mesh contraction, and tissue response to a novel omega-3 fatty acid bioabsorbable barrier macroporous mesh after intraperitoneal placement. Surg Innov 2009;16: 46–54.
29. Scheller B, Unverdorben M, Vallbracht C, Cremers B, Heuer H, Hengstenberg C, Maikowski C, Werner GS, Antoni D, Kleber FX, Bocksch W, Leschke M, Ackermann H, Boxberger M, Speck U, Degenhardt R, Scheller B. Treatment of coronary in-stent restenosis with a paclitaxel-coated balloon catheter. N Engl J Med 2006; 355:2113–2124.
30. Sgueglia GA, Todaro D, Bisciglia A, Conte M, Stipo A, Pucci E. Kissing inflation is feasible with all second-generation drug-eluting balloons. Cardiovasc Revasc Med, 2011.